Published in final edited form as:
J Biomater Appl. 2013 February ; 27(6): 695–705. doi:10.1177/0885328211423783.

Nanofiber Scaffold Gradients for Interfacial Tissue Engineering

Murugan Ramalingam[a,b,c], **Marian F. Young**[b], **Vinoy Thomas**[d,e], **Limin Sun**[f], **Laurence C. Chow**[f], **Christopher K. Tison**[a], **Kaushik Chatterjee**[a,b], **William C. Miles**[a], and **Carl G. Simon Jr.**[a]

Carl G. Simon: carl.simon@nist.gov

[a]Polymers Division, National Institute of Standards and Technology, 100 Bureau Drive, Gaithersburg, MD 20899 (U.S.A.)

[b]National Institute of Dental and Craniofacial Research, National Institutes of Health, Bethesda, MD 20892 (USA)

[c]National Institute of Health and Medical Research, Faculty of Medicine, University of Strasbourg, 67085 Strasbourg Cedex (France)

[d]Ceramics Division, National Institute of Standards and Technology, Gaithersburg, MD 20899 (U.S.A.)

[e]Center for Nanoscale Materials & Biointegration, University of Alabama at Birmingham, Birmingham, AL 35294 (U.S.A.)

[f]American Dental Association, Paffenbarger Research Center, National Institute of Standards and Technology, Gaithersburg, MD 20899 (U.S.A.)

Abstract

We have designed a 2-spinnerette device that can directly electrospin nanofiber scaffolds containing a gradient in composition that can be used to engineer interfacial tissues such as ligament and tendon. Two types of nanofibers are simultaneously electrospun in an overlapping pattern to create a nonwoven mat of nanofibers containing a composition gradient. The approach is an advance over previous methods due to its versatility - gradients can be formed from any materials that can be electrospun. A dye was used to characterize the 2-spinnerette approach and applicability to tissue engineering was demonstrated by fabricating nanofibers with gradients in amorphous calcium phosphate nanoparticles (nACP). Adhesion and proliferation of osteogenic cells (MC3T3-E1 murine pre-osteoblasts) on gradients was enhanced on the regions of the gradients that contained higher nACP content yielding a graded osteoblast response. Since increases in soluble calcium and phosphate ions stimulate osteoblast function, we measured their release and observed significant release from nanofibers containing nACP. The nanofiber-nACP gradients fabricated herein can be applied to generate tissues with osteoblast gradients such as ligaments or tendons. In conclusion, these results introduce a versatile approach for fabricating nanofiber gradients that can have application for engineering graded tissues.

Keywords

Nanofibers; Scaffolds; Calcium Phosphate; Gradient; Osteoblast

Correspondence to: Carl G. Simon, Jr., (T: 301-975-8574; F: 301-975-4977; carl.simon@nist.gov).
Dedicated to the memory of Janet B. Quinn, Ph.D.

Introduction

Strategies for patterning cells and tissues are in high demand for replicating the hierarchical structures found in tissue and organs (1–4). Organs contain multiple tissues that must interface with one another and can contain gradients in cells, growth factors, extracellular matrix proteins or physical properties. During development, gradients in morphogens are critical for pattern formation and generation of limbs (1). Ligaments and tendons link soft and hard tissues and contain a gradation from calcified to non-calcified tissue (2). Patterned scaffolds that can drive generation of patterned tissues could be used to tissue engineer these hierarchical structures (3;4). In order to advance methods for generating interface tissues, we have previously developed methods for fabricating 3D scaffold gradients for salt-leached scaffolds (5) and hydrogels (4). Herein, we focus on nanofibers. Electrospun nanofiber scaffolds have shown promise because they mimic the nanotopography of native extracellular matrices (6;7). We have developed a 2-spinnerette approach for fabricating nanofiber scaffolds with composition/property gradients.

Two spinnerettes were placed side-by-side to dispense simultaneously two different types of nanofibers that lay down in an overlapping pattern to create a gradient in nanofiber composition. The device and gradient fabrication were characterized using dyes and absorbance measurements. To demonstrate the application of the nanofiber gradients, an orthopaedic tissue engineering model was used using polymeric nanofibers with gradients in amorphous calcium phosphate nanoparticles (nACP). Poly(ε-caprolactone) (PCL) scaffolds can support osteogenesis (8;9) while calcium phosphates are osteoconductive (8;10–12). Calcium phosphate biomaterials can elicit their effects by releasing calcium ions which stimulate osteoblast proliferation through a calcium receptor or by releasing phosphate ions which stimulate osteoblast differentiation (13;14). Nanofibers with nACP gradients were fabricated and used to screen adhesion (1 d) and proliferation (7 d) of the MC3T3-E1 murine calvarial osteoblast cell line, a well-characterized in vitro model for osteoblasts (15). The results show that the nACP-nanofiber gradients can induce a graded osteoblast response which can have application for engineering graded tissues such as ligament or tendon.

Materials and methods

Sudan IV nanofiber library

A new 2-spinnerette approach was developed that deposits two different polymer solutions into a non-woven mat composed of a mix of two nanofiber types in the form of a gradient. The new method was characterized by fabricating gradients of Sudan IV red dye and measuring absorbance to determine composition. PCL (relative molecular mass 80000 g/mol) was used to fabricate scaffold libraries using 10% (mass/volume, 1 g PCL in 10 mL solvent) solutions in 3:1 chloroform:methanol (volume ratio). One spinnerette spun PCL fibers (clear) while the second spinnerette spun PCL fibers with Sudan IV (0.03% mass/volume) (red). Two beveled syringe tips (18 gauge, 10 cm) with bevels facing each other were used as spinnerettes. Spinnerettes were 2.5 cm apart and oriented vertically 17 cm above the target (aluminum foil, 32.5 cm × 33.5 cm). The spinnerettes were offset in the z-direction (vertical) so that the red spinnerette was 3 mm lower than the clear one. The flow rate was 2 mL/h per spinnerette (4 mL/h total) with voltage 16 kV (24°C, 50% relative humidity) for a 1 h spin time. The ground was attached to the foil target. An insulated wire connected the two spinnerettes and was bared in the middle where it was connected to the positive lead from the power supply. Spinnerettes were mounted with plastics (no metal within 10 cm of the spinnerettes) since metals interfered with the electric field causing inconsistent gradients. The process repeatably yielded a gradient (17 cm × 6 cm). The nanofiber scaffold libraries were cut into sections (0.5 cm × 6 cm), sections were dissolved in solvent (3:1 chloroform:methanol) and dye absorbance was determined

spectrophotometrically (plate-reader, 440 nm). Control nanofiber scaffolds of uniform composition of either pure “clear” (PCL) or pure “red” (PCL with red dye) were analyzed as controls. To generate control nanofiber mats, the 2-spinnerette system was used with the same solution in both syringes.

Preparation of nACP

Amorphous calcium phosphate nanoparticles (nACP) with Ca:P molar ratio of 1.5 were prepared by a spray-drying process (16). Briefly, calcium carbonate and dicalcium phosphate were dissolved in acetic acid solution at a 1.5 Ca:P ratio. The solution was sprayed through a nozzle (SUC1120, PNR America) on a glass column. Filtered air was drawn from the top of the column, which removed volatile acid and water from the sprayed liquid generating fine particles suspended in the airflow which were collected using an electrostatic precipitator. nACP crystallinity was assessed by powder X-ray diffraction (Rigaku DMAX 2200, 2θ uncertainty was 0.01°). nACP morphology was assessed by transmission electron microscopy (Philips EM-400T field-emission-gun TEM, accelerating voltage 120 kV) where nACP particles were dispersed in acetone by sonication and analyzed after deposition onto amorphous carbon-coated copper grids.

nACP-nanofiber gradients

Nanofiber scaffolds with gradients in nACP were fabricated. One syringe was loaded with PCL (10 % mass/vol.; 1 g PCL + 10 mL of 3:1 chloroform:methanol) while the second syringe was loaded with a PCL/nACP solution (1 g PCL + 0.43 g nACP + 10 mL 3:1 chloroform:methanol). Gradients were fabricated as described above (22 cm × 6 cm). For characterization, gradients were cut into sections (0.5 cm × 6 cm, 5 mg) and nACP content was quantified by thermogravimetric analysis (TGA) (10°C/min, 30°C to 600°C, under nitrogen, TA Instruments Q500). The residual mass percent at 592°C was used as nACP composition. Control nanofiber scaffolds of uniform composition of PCL or PCL-nACP were prepared for some experiments using the 2-spinnerette system (same solution was loaded into both syringes). Nanofiber scaffold morphology was assessed by scanning electron microscopy of sputter-coated (gold) specimens (15 kV, Hitachi S-4700-II FE-SEM).

Cell culture

For cell culture, scaffold libraries were cut into 4 gradient strips (1.5 cm × 22 cm), affixed 8 strips per dish (24.5 cm × 24.5 cm plastic dishes, non-tissue culture treated) using silicone vacuum grease, sterilized with ethylene oxide and degassed 2 d in a desiccator under vacuum. MC3T3-E1 murine pre-osteoblasts (Riken Cell Bank) were cultured in α-modification of Eagle’s minimum essential medium (α-MEM, Cambrex Bio Science) supplemented with 10% fetal bovine serum (Gibco) and 0.060 mg/mL kanamycin sulfate (Sigma) (15;17). The medium was changed twice weekly and cultures were passaged with 2.5 g/L trypsin (0.25% mass fraction) containing 1 mmol/L EDTA (ethylenedinitrilotetraacetic acid; Gibco). Cells passaged four times after receipt from Riken and at 80 % confluency were used for all experiments. Seven million cells in 175 mL medium were seeded into each dish (12000 cells/cm^2), left undisturbed for 1 h to allow cell attachment and moved to the incubator for 1 d or 7 d culture (medium change at 3 d).

Cell assays

A total of 8 PCL-nACP gradient strips (1.5 cm × 22 cm) were used for the cell culture experiments: four of each for 1 d and 7 d. After cell culture and at appropriate time points (1 d or 7 d), each strip was cut into 14 sections for cell assays. The 2 end pieces were discarded, 6 sections were used for fluorescence microscopy (Sytox green) and 6 were used

for Picogreen DNA assay. For fluorescence imaging, sections were fixed for 5 min [0.5% mass fraction Triton X-100, 4% mass fraction paraformaldehyde, 5% mass fraction sucrose, 1 mmol/L $CaCl_2$, 2 mmol/L $MgCl_2$ in phosphate buffered saline (PBS), pH 7.4], post-fixed for 20 min (same as fix but without Triton X-100), blocked for 1 h (1% mass fraction bovine serum albumin) and stained 1 h in PBS containing 5 μmol/L Sytox green (green nuclei) (Invitrogen). Wet scaffolds were imaged using inverted epifluorescence microscopy. For Picogreen DNA assay, scaffold sections were incubated overnight with lysis buffer [1 mL, 0.2 mg/mL Proteinase K (19 Units/mg; Sigma), 0.2 mg/mL sodium dodecyl sulfate (0.02 % mass/vol) in PBS] at 37°C. One mL of the lysates was transferred to a 96-well plate, diluted 1:1 with a 200-fold dilution of the Picogreen reagent (Invitrogen) and fluorescence measured by plate-reader (excitation 485 nm; emission 538 nm). A DNA standard curve was prepared for calibration.

Calcium and phosphate ion release

Control PCL or PCL-nACP nanofibers (15 mg of nanofibers) were added to 4 mL of cell medium (with serum) containing 10 mM HEPES (4-(2-hydroxyethyl)-1-piperazineethanesulfonic acid) (pH 7.4). After 15 min at 37 °C with stirring (250 rpm), solutions were filtered (0.22 μm) for analysis of calcium and phosphate concentrations using spectrophotometric methods (18). Blank solutions (no nanofibers) were used as controls to determine background.

Results

The 2-spinnerette system (Fig. 1) was characterized by making PCL nanofiber scaffolds containing red dye (Sudan IV) gradients since the red dye is visible and can be quantified by absorbance measurements. Gradients were cut into sections and the red dye absorbance was measured to assess gradient generation. A plot of composition versus position for five red dye gradients each fabricated on a different day demonstrates the efficiency and repeatability of the custom-designed 2-spinnerette device (Fig. 2).

Getting repeatable gradients was challenging and a number of key parameters were identified that made the 2-spinnerette device effective. First, there cannot be any drafts. Electrospinning devices are commonly assembled in a hood (for solvent), but the draw of air into the hood leads to uneven fiber deposition and irregular gradients. Our unit was installed on a bench top, away from foot traffic and was enclosed in plexiglass to shield from drafts. Second, there can be no metal parts (not even clamps) within 10 cm of the spinnerettes (only plastic or wood). Metal causes shorts and interferes with the electric field causing irregular electrospinning. Third, an insulated wire was used to connect the two spinnerettes to the power supply (Fig. 2). This was critical to reduce the repulsion between the two spinnerettes so that the fiber jets would overlap and create a gradient. Fourth, having beveled syringe tips with bevels facing each other for the two spinnerettes and having the two spinnerettes offset 3 mm in the z-direction were essential for getting gradients. Without these modifications, the two streams repelled one another and their overlap was minimal (no gradient). Thus, optimization of the 2-spinnerette design was demanding but several modifications were implemented that made the device effective and reliable.

Next, nanofiber scaffolds with gradients of nACP were fabricated to demonstrate application of nanofiber gradients for tissue engineering. nACP powder was characterized by X-ray diffraction (XRD) and transmission electron microscopy (TEM) (Fig. 3) which showed that the nACP powder was amorphous and that it consisted of nano-sized particles (≈100 nm). Scanning electron microscopy was used to examine the morphology of the nanofiber scaffolds (Fig. 3). Control PCL and PCL-nACP nanofibers had a similar morphology and a similar fiber diameter. nACP particles were visible on the surface of the control PCL-nACP

nanofibers. The morphology and diameter of nanofibers with nACP gradients was similar to control nanofibers (not shown). In addition, little nACP was seen on fibers from nACP-poor regions of the gradients while more nACP was visible on fibers from nACP-rich regions of the gradients. Thermogravimetric analysis (TGA) yielded the composition of PCL-nACP nanofiber gradient scaffolds. Gradients fabricated on 3 different days had similar compositional profiles demonstrating the repeatability of the nACP gradient fabrication approach (Fig. 4).

MC3T3-E1 osteoblasts were cultured on gradient nanofibers and fluorescence microscopy and the Picogreen DNA assay were used to assess cell response. Both cell adhesion (1 d) and proliferation (7 d) were enhanced on nACP-rich regions of the nanofiber gradients compared to the nACP-poor regions of the gradient (Fig. 5). Increased cell numbers were detected with increasing nACP content by both fluorescence microscopy and by DNA assay. Statistical testing showed that differences in cell adhesion and proliferation were significant ($P < 0.05$). Control experiments using nanofiber specimens without gradients (uniform composition) were used to validate the gradient results (Fig. 6). Cell numbers after 1 d and 7 d culture were significantly higher on control PCL-nACP nanofibers than on control PCL nanofibers ($P < 0.05$). Thus, nACP potentiated osteoblast adhesion (1 d) and proliferation (7 d) for both gradient and control nanofiber formats, which validates the gradient approach.

To explore the mechanism whereby PCL-nACP nanofibers promoted osteoblast function, the release of calcium and phosphate ions from nanofibers was measured (Fig. 7). PCL-nACP nanofibers caused a significant increase in soluble calcium and phosphate concentration ($P < 0.05$) when incubated in cell medium whereas control PCL nanofibers did not ($P > 0.05$). These results show that nACP in the nanofibers partially dissolved during cell culture to release ions of calcium and phosphate which could stimulate osteoblast function. Calcium and phosphate ions have previously been shown to stimulate osteoblast proliferation and differentiation (13;14) and an increase in these ions caused by nACP dissolution would be expected to do the same.

Discussion

Gradient nanofiber scaffolds can have application for engineering graded tissues (2–4). Ligaments and tendons join soft and hard tissues utilizing gradients from collagenous, fibrous tissue into hard bony tissue (2;3). The tendon to bone interface contains a gradation from non-calcified to calcified tissue (2). The PCL-nACP nanofiber gradients fabricated herein induced a graded response in osteoblast adhesion and proliferation that could mimic these calcification gradients. The effective length of the current PCL-nACP nanofiber gradients ran from 4 cm to 17 cm as shown in Fig. 4 (13 cm in length). For repair of Achilles tendon, 12 cm contructs have been used (19). In addition, 10 cm grafts have been used for ligament reconstruction of the thumb (20). Thus, the current PCL-nACP nanofiber gradients are in the appropriate size range for repairing Achilles tendon or thumb ligament in humans.

Other methods for fabricating nanofiber gradients have been demonstrated for inducing a graded cell response including methods where successive layers of different nanofibers were spun into a layered mat (10;21), assembly of nanofiber gradients were directed by a magnetic field (22) and nanofiber matts were differentially exposed to a reactive solution (11;23). These other approaches required modification of nanofibers after electrospinning while the 2-spinnerette method described herein yields gradients directly. In addition, the 2-spinnerette approach is more versatile and can yield nanofiber gradients from any materials that can be elctrospun (polymers, composites, nanoparticles, growth factors, peptides, etc.).

Conclusions

In summary, a versatile 2-spinnerette method for fabricating nanofiber scaffolds with gradients in composition has been introduced that can be used to fabricate nanofiber gradients from any materials that can be electrospun. Several key device modifications were identified that make the approach reliable and effective. Application of the nanofiber gradients to tissue engineering was demonstrated by making gradients in nACP composition. Nanofiber scaffolds with gradients in nACP induced a graded response in osteoblast adhesion and proliferation. These results show that nACP nanofiber gradients can have application for engineering interface tissues such as ligaments or tendons which contain osteoblast gradients.

Acknowledgments

M.R., V.T. and K.C. acknowledge National Academies/NRC NIBIB/NIH-NIST Postdoctoral Fellowship program (National Research Council, National Institute of Biomedical Imaging and Bioengineering, National Institutes of Health). We thank G. Christopherson for help with figures. This work was supported by NIST, NIH/NIBIB R21 EB006497-01, NIH-NIDCR R01 DE16416 and the Intramural Program of the NIH/NIDCR (National Institute of Dental and Craniofacial Research). The “standard deviation” (S.D.) is the same as the “combined standard uncertainty of the mean” for the purposes of this work. The content is solely the responsibility of the authors and does not necessarily represent the official views of NIH, ADA (American Dental Association), NIBIB, NIDCR or NIST. This article, a contribution of NIST, is not subject to US copyright. Certain equipment and instruments or materials are identified in the paper to adequately specify the experimental details. Such identification does not imply recommendation by NIST, nor does it imply the materials are necessarily the best available for the purpose.

References

1. Affolter M, Basler K. The Decapentaplegic morphogen gradient: from pattern formation to growth regulation. Nat. Rev. Genet. 2007; 8(9):663–674. [PubMed: 17703237]
2. Moffat KL, Sun WH, Pena PE, et al. Characterization of the structure-function relationship at the ligament-to-bone interface. Proc. Natl. Acad. Sci. U. S. A. 2008; 105(23):7947–7952. [PubMed: 18541916]
3. Phillips JE, Burns KL, Le Doux JM, Guldberg RE, Garcia AJ. Engineering graded tissue interfaces. Proc. Natl. Acad. Sci. U. S. A. 2008; 105(34):12170–12175. [PubMed: 18719120]
4. Chatterjee K, Lin-Gibson S, Wallace WE, et al. The effect of 3D hydrogel scaffold modulus on osteoblast differentiation and mineralization revealed by combinatorial screening. Biomaterials. 2010; 31(19):5051–5062. [PubMed: 20378163]
5. Chatterjee K, Sun L, Chow LC, Young MF, Simon CG Jr. Combinatorial screening of osteoblast response to 3D calcium phosphate/poly(epsilon-caprolactone) scaffolds using gradients and arrays. Biomaterials. 2011; 32(5):1361–1369. [PubMed: 21074846]
6. Li WJ, Danielson KG, Alexander PG, Tuan RS. Biological response of chondrocytes cultured in three-dimensional nanofibrous poly(epsilon-caprolactone) scaffolds. Journal of Biomedical Materials Research Part A. 2003; 67A(4):1105–1114. [PubMed: 14624495]
7. Christopherson GT, Song H, Mao HQ. The influence of fiber diameter of electrospun substrates on neural stem cell differentiation and proliferation. Biomaterials. 2009; 30(4):556–564. [PubMed: 18977025]
8. Wutticharoenmongkol P, Pavasant P, Supaphol P. Osteoblastic phenotype expression of MC3T3-E1 cultured on electrospun polycaprolactone fiber mats filled with hydroxyapatite nanoparticles. Biomacromolecules. 2007; 8(8):2602–2610. [PubMed: 17655356]
9. Kim K, Lee CH, Kim BK, Mao JJ. Anatomically shaped tooth and periodontal regeneration by cell homing. J. Dent. Res. 2010; 89(8):842–847. [PubMed: 20448245]
10. Erisken C, Kalyon DM, Wang H. Functionally graded electrospun polycaprolactone and beta-tricalcium phosphate nanocomposites for tissue engineering applications. Biomaterials. 2008; 29(30):4065–4073. [PubMed: 18649939]

11. Li XR, Xie JW, Lipner J, et al. Nanofiber Scaffolds with Gradations in Mineral Content for Mimicking the Tendon-to-Bone Insertion Site. Nano Letters. 2009; 9(7):2763–2768. [PubMed: 19537737]
12. Nandakumar A, Yang L, Habibovic P, van BC. Calcium phosphate coated electrospun fiber matrices as scaffolds for bone tissue engineering. Langmuir. 2010; 26(10):7380–7387. [PubMed: 20039599]
13. Yamaguchi T, Chattopadhyay N, Kifor O, et al. Mouse osteoblastic cell line (MC3T3-E1) expresses extracellular calcium (Ca2+o)-sensing receptor and its agonists stimulate chemotaxis and proliferation of MC3T3-E1 cells. J. Bone Miner. Res. 1998; 13(10):1530–1538. [PubMed: 9783541]
14. Beck GR Jr, Zerler B, Moran E. Phosphate is a specific signal for induction of osteopontin gene expression. Proc. Natl. Acad. Sci. U. S. A. 2000; 97(15):8352–8357. [PubMed: 10890885]
15. Sudo H, Kodama HA, Amagai Y, Yamamoto S, Kasai S. In vitro differentiation and calcification in a new clonal osteogenic cell line derived from newborn mouse calvaria. J. Cell Biol. 1983; 96(1):191–198. [PubMed: 6826647]
16. Chow LC, Sun LM, Hockey B. Properties of nanostructured hydroxyapatite prepared by a spray drying technique. Journal of Research of the National Institute of Standards and Technology. 2004; 109(6):543–551.
17. Simon CG, Eidelman N, Kennedy SB, et al. Combinatorial screening of cell proliferation on poly(D,L-lactic acid)/poly(D,L-lactic acid) blends. Biomaterials. 2005; 26(34):6906–6915. [PubMed: 15939467]
18. Vogel GL, Chow LC, Brown WE. A microanalytical procedure for the determination of calcium, phosphate and fluoride in enamel biopsy samples. Caries Res. 1983; 17(1):23–31. [PubMed: 6571804]
19. Demirel M, Turhan E, Dereboy F, Yazar T. Augmented repair of acute tendo Achilles ruptures with gastrosoleus turn down flap. Indian. J. Orthop. 2011; 45(1):45–52. [PubMed: 21221223]
20. Kokkalis ZT, Zanaros G, Sotereanos DG. Ligament reconstruction with tendon interposition using an acellular dermal allograft for thumb carpometacarpal arthritis. Tech. Hand Up Extrem. Surg. 2009; 13(1):41–46. [PubMed: 19276927]
21. Thomas V, Zhang X, Catledge SA, Vohra YK. Functionally graded electrospun scaffolds with tunable mechanical properties for vascular tissue regeneration. Biomed. Mater. 2007; 2(4):224–232. [PubMed: 18458479]
22. Valmikinathan CM, Wang JP, Smiriglio S, Golwala NG, Yu XJ. Magnetically Induced Protein Gradients on Electrospun Nanofibers. Combinatorial Chemistry & High Throughput Screening. 2009; 12(7):656–663. [PubMed: 19531021]
23. Shi J, Wang L, Zhang F, et al. Incorporating protein gradient into electrospun nanofibers as scaffolds for tissue engineering. ACS Appl. Mater. Interfaces. 2010; 2(4):1025–1030. [PubMed: 20423122]

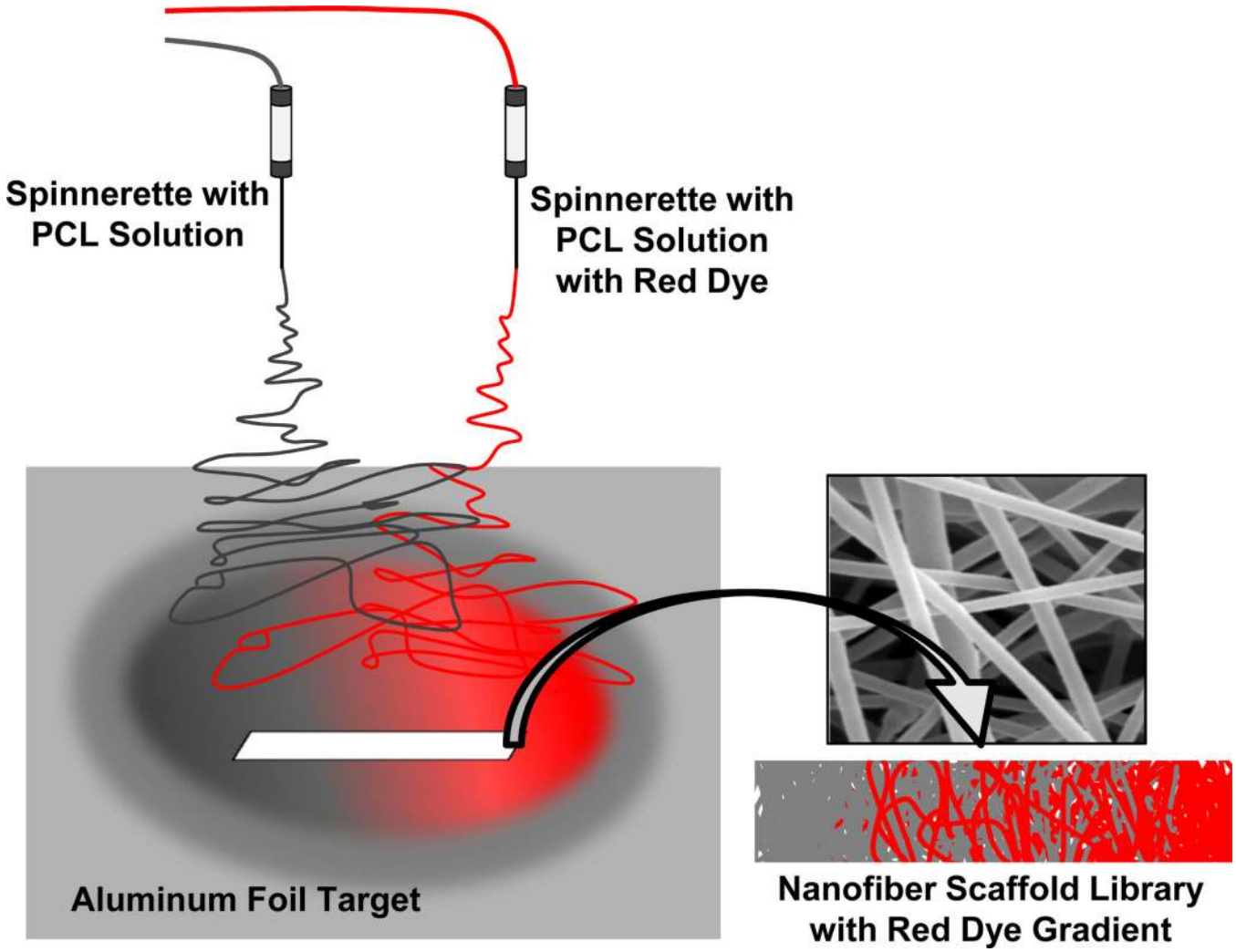

Figure 1.
Scheme of 2-spinnerette approach for fabricating nanofiber scaffold gradients.

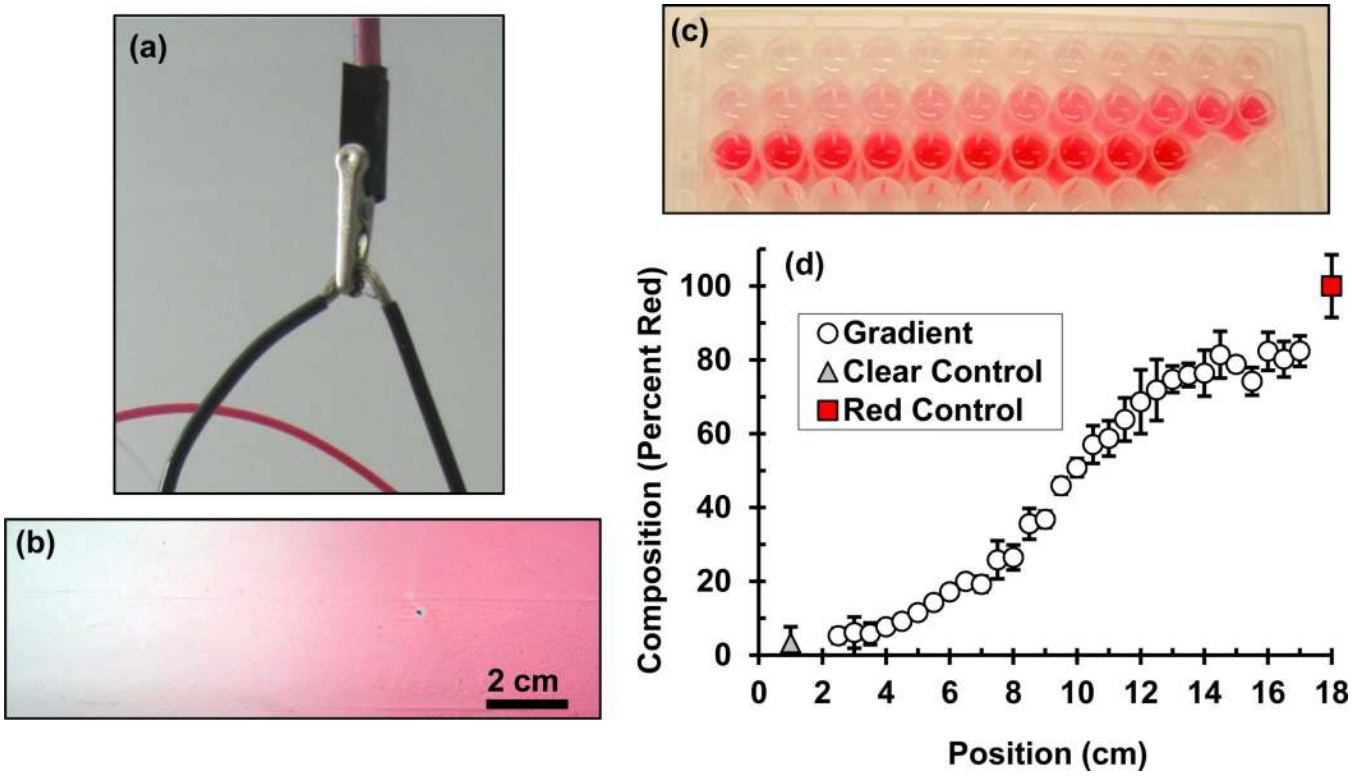

Figure 2.

(a) Photograph of wire connecting lead from power supply to the spinnerettes. A short piece of insulated wire (10 cm) was bared in the middle to connect to the power supply and the two ends of the wire were attached to the two spinnerettes. (b) Photograph of nanofiber scaffold gradient fabricated using two PCL solutions where one contained red dye. (c,d) Absorbance (440 nm) of dissolved scaffold sections were measured with a plate-reader to characterize the nanofiber gradient composition. Five libraries (17 cm × 6 cm) fabricated on different days were analyzed (n = 5). Error bars are S.D.

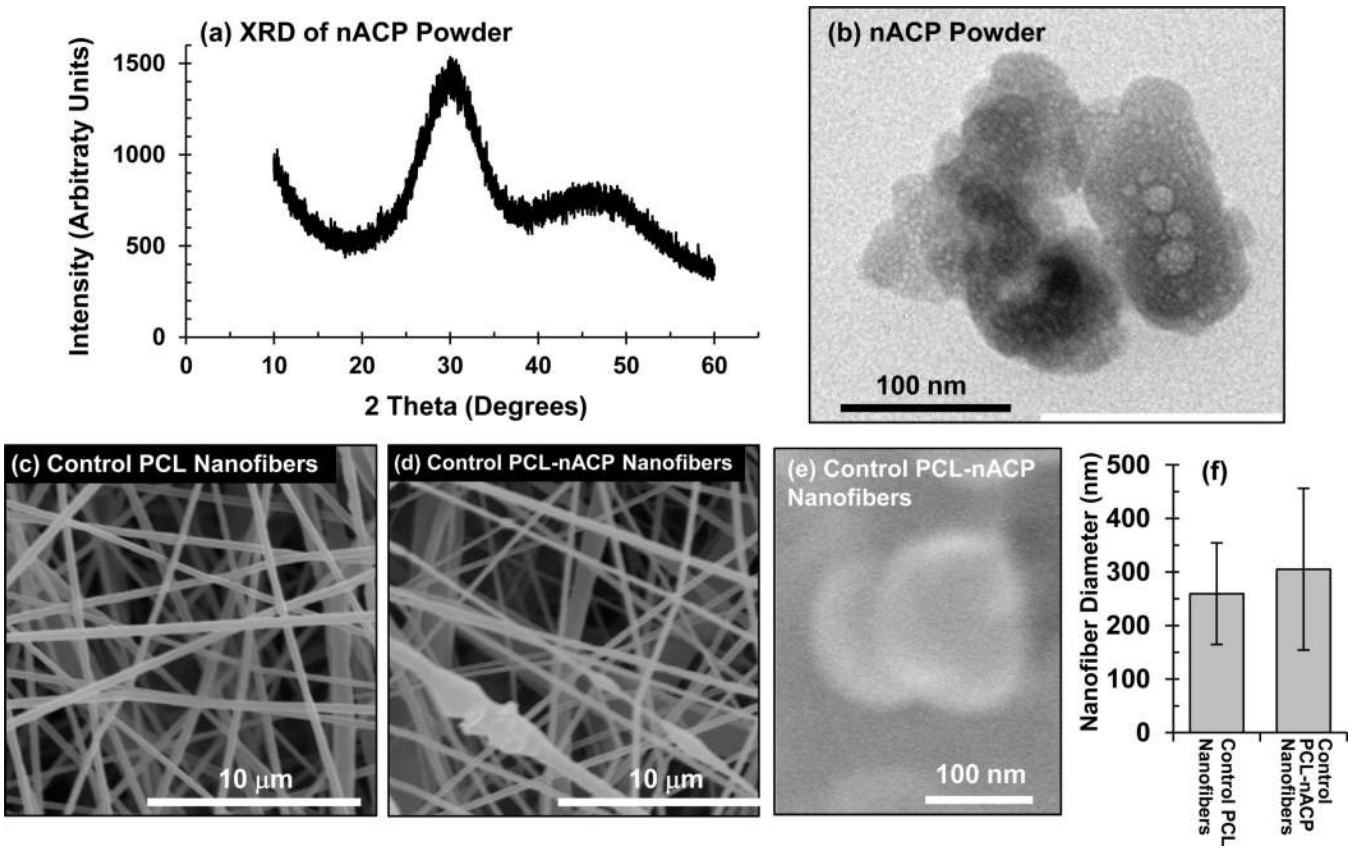

Figure 3.

(a) XRD of nACP powder. (b) TEM of nACP particles. (c,d) SEM of control PCL (0 mass percent nACP) and PCL-nACP nanofibers (24 mass percent nACP). (e) Higher magnification SEM showing nACP particle on the surface of a control PCL-nACP nanofiber. (f) The diameter of control PCL and PCL-nACP nanofibers as determined by SEM (error bars are S.D., n = 10) are not significantly different [t-test, $P > 0.05$].

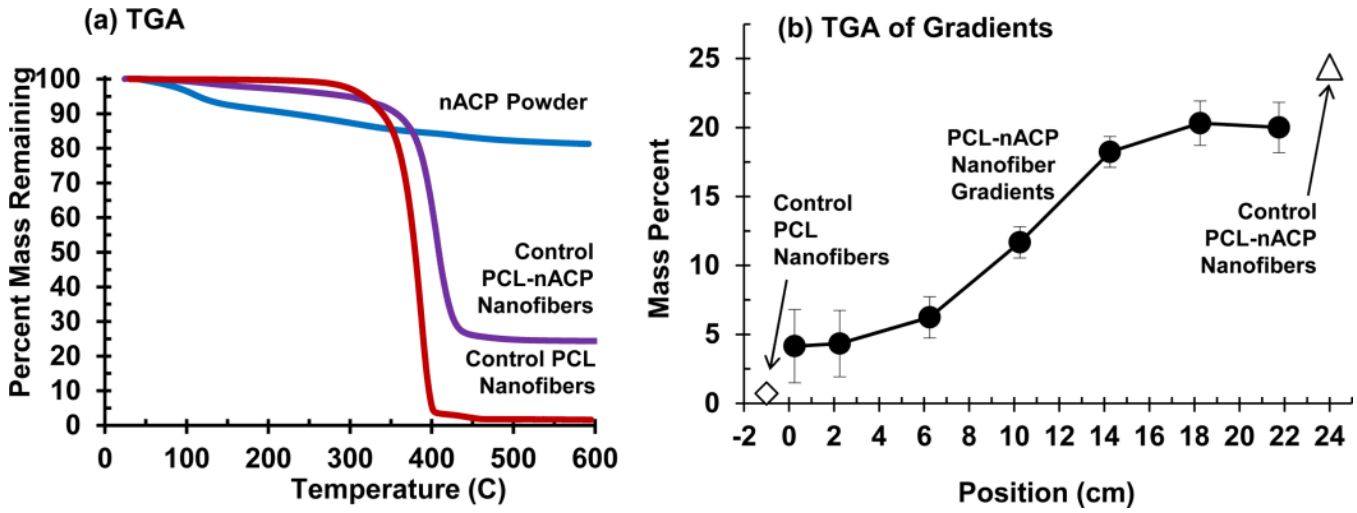

Figure 4.

(a) Thermogravimetric traces (TGA) of nACP powder, control PCL-nACP nanofibers (24 mass percent nACP) and control PCL nanofibers (0 mass percent nACP). PCL burns off during heating while nACP is stable, enabling determination of nACP content in PCL-nACP nanofibers. (b) nACP composition of nanofiber scaffolds determined by TGA. Solid circles are PCL-nACP nanofiber gradients (n = 3), open diamond is control PCL nanofibers (n = 5) and open triangle is control PCL-nACP nanofibers (n = 3). Error bars are S.D.

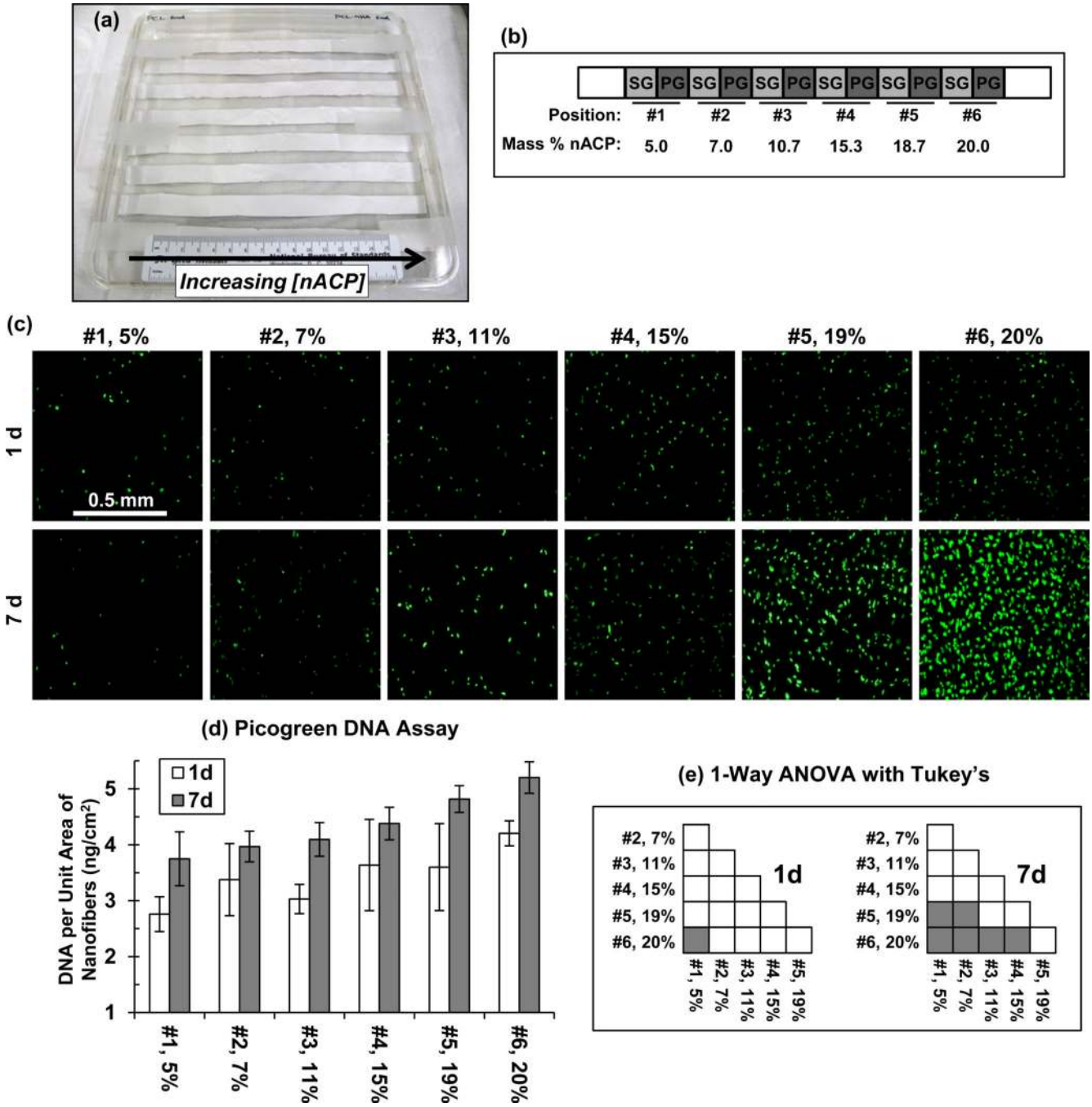

Figure 5.

(a) Photograph of eight PCL-nACP nanofiber gradients (22 cm × 1.5 cm strips) in a cell culture dish. (b) Nanofiber gradients were analyzed with cell culture assays. After culture, the two end sections were discarded (white) while the middle part was cut into 12 sections (1.5 cm × 1.5 cm) where 6 were used for Sytox green ("SG", light grey) and 6 were used for Picogreen DNA assay ("PG", dark grey). Note that SG and PG sections were paired into 6 positions and the nACP compositions are given. Compositions were determined from Fig. 4b and the values are used in other figures. (c) Fluorescence images of green-stained nuclei of MC3T3-E1 osteoblasts cultured 1 d or 7 d on PCL-nACP nanofiber gradients. Scale bar applies to all images. Numbers indicate gradient position and mass percent nACP. (d)

Picogreen DNA assay for cells cultured on PCL-nACP nanofiber gradients for 1 d or 7 d. Error bars are S.D. (n = 4). (e) Statistical analysis for Picogreen DNA data. Grey shaded boxes indicate significant differences for DNA amount from different positions in the nanofiber gradients (ANOVA with Tukey's, $p < 0.05$).

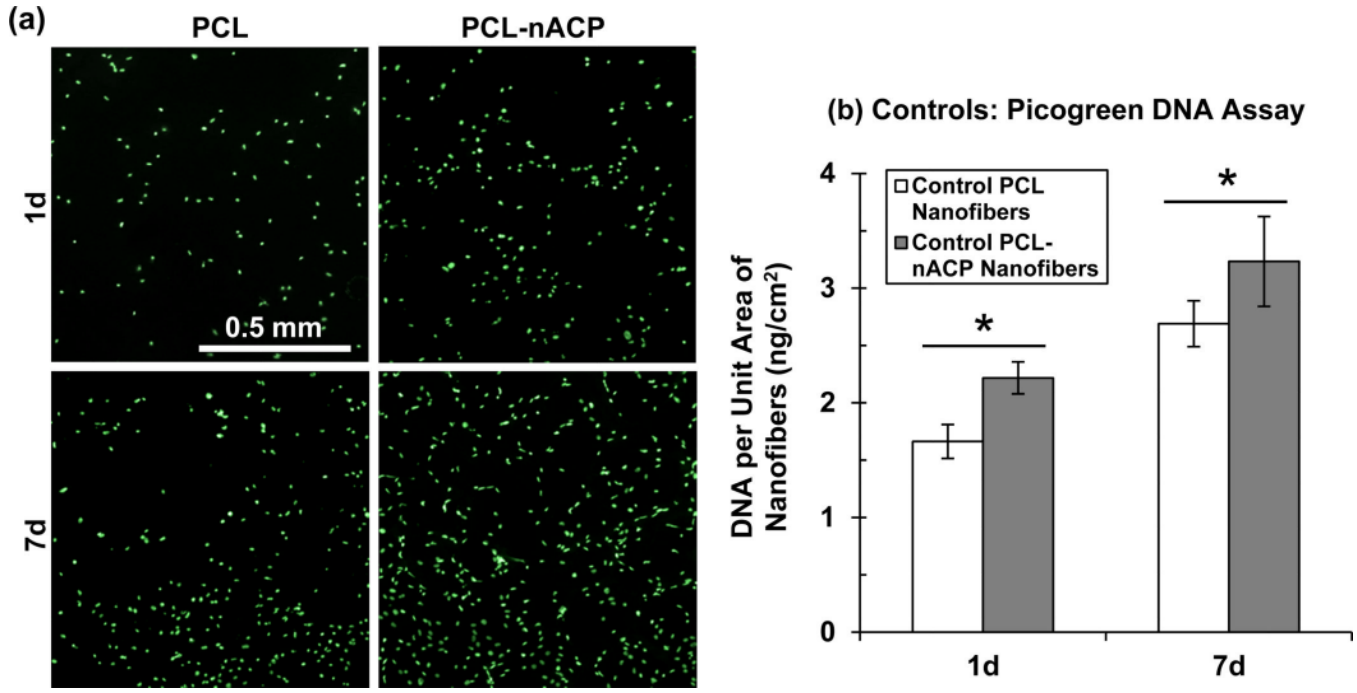

Figure 6.

Control cell experiments using nanofiber specimens with uniform composition to validate gradient experiments. (a) Fluorescence images of Sytox green stained nuclei of MC3T3-E1 cells cultured 1 d or 7 d on control PCL nanofibers or control PCL-nACP nanofibers. The scale bar applies to all images in (a). (b) Picogreen DNA assay for cells cultured on control PCL nanofibers (0 mass percent nACP) or control PCL-nACP nanofibers (24 mass percent nACP) for 1 d or 7 d. Error bars are S.D. (n = 12). Asterisks indicate significant differences (t-test, $P < 0.05$).

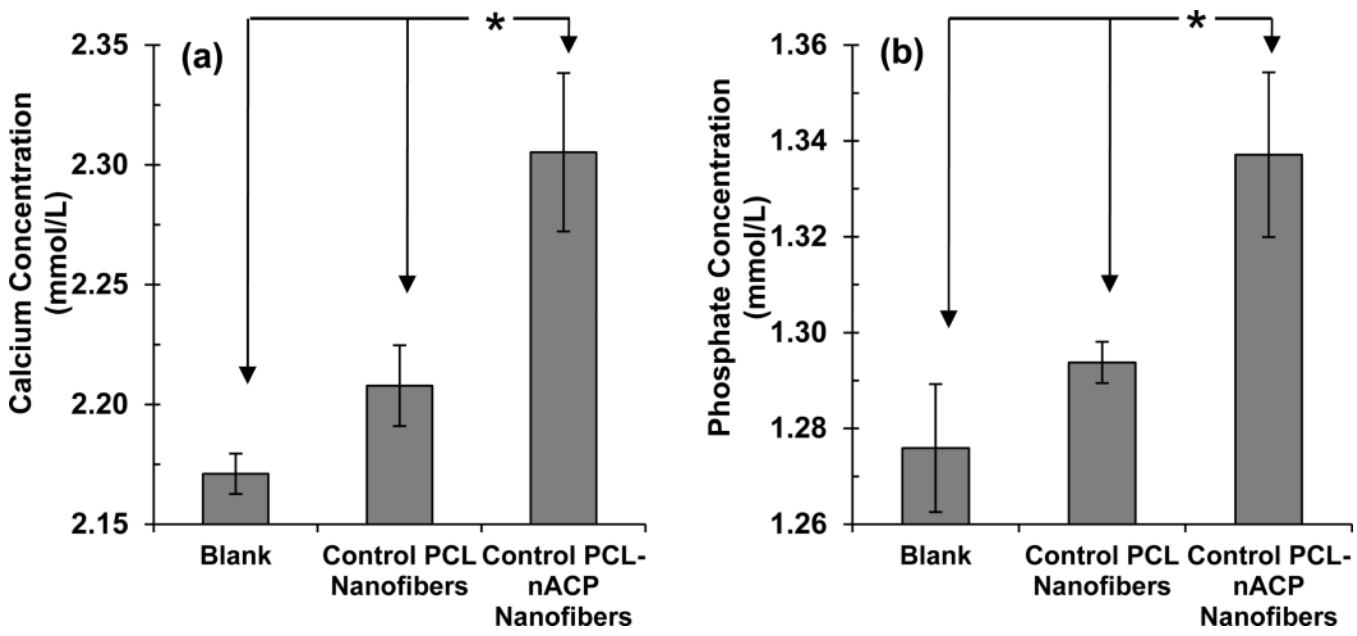

Figure 7.

Change in calcium (a) and phosphate (b) concentration in cell medium after 15 min incubation with control PCL nanofibers (0 mass percent) or control PCL-nACP nanofibers (8 mass percent nACP). Error bars are S.D. (n = 3). Asterisks indicate that PCL-nACP nanofiber values were significantly different from blank controls and PCL nanofibers (1-way ANOVA with Tukey's, $P < 0.05$).